Ocean Science Journal manuscript No.
(will be inserted by the editor)

Experiments on surface waves interacting with flexible aquatic vegetation

Luca Cavallaro · Antonino Viviano · Giovanni Paratore · Enrico Foti

Received: 21 November 2017

Abstract Surface wave interaction with aquatic vegetation appears to play a key role in coastal hydro-morpho-dynamics. As an example, the presence of a dense meadow at intermediate water depth is usually associated with a stable and resilient shore. Wave-meadow interactions are investigated here by means of physical modeling, with a focus on wave height distribution and hydrodynamics. The central part of a wave flume is covered by flexible artificial seagrass, composed of polyethylene leaves. This vegetation is tested in both near emergent and submerged conditions.

The wave height reduction is evaluated by means of a drag coefficient defined from linear wave theory, which contains all the unknowns of the adopted

L. Cavallaro, A. Viviano, G. Paratore, E. Foti

Department Civil Engineering and Architecture, University of Catania, Catania, Italy

Tel.: +039-095-7382701

Fax: +039-095-7382748

E-mail: luca.cavallaro@dica.unict.it

methodology. The behaviour of such a coefficient is investigated as a function of a wave related Reynolds number. The influence of the flexibility of the leaves is also considered, together with a wave frequency parameter. The results show a complex behavior with three different trends for near rigid, intermediate or highly flexible leaves.

Amplitudes of the orbital velocities are investigated and show a fairly good match with the linear wave theory. On the contrary, the mean velocity along the water column appears to be modified by the seagrass for submerged leaves.

Keywords water waves · vegetation · hydrodynamics

1 Introduction

The aquatic vegetation causes important effects on the coastal ecosystem and hydrodynamics, especially in the shallow waters where the length of the plants is similar to the water depth. Indeed, the aquatic vegetation has structural and functional consequences for the environment by resisting the flow and modifying the flow locally (Carpenter and Lodge, 1986; Bouma et al, 2005; Peralta et al, 2006). Seagrass meadows play a great role in maintaining biodiversity since they favor the growth of algae, fish and invertebrates. Seagrasses play a relevant role in coastal protection since they increase bottom roughness, thus reducing near-bed velocity and modifying the sediment transport and increasing the wave attenuation. Furthermore, vegetation may influence the coastal risk by altering the wave propagation on beach (John et al, 2016) and the load on coastal structures (Lakshmanan et al, 2012).

However, the interaction between vegetation and flow has not been clear up to now, especially when integrated into a wave propagation model.

Such an interaction is amplified in the presence of flexible plants since seagrass and waves affect each other in highly coupled, nonlinear ways (Koch et al, 2006). As a result of this interaction, seagrass represents a variable hydraulic roughness: as the flow velocity increases the leaves increasingly bend, until they eventually lie on the bottom. Therefore, the roughness has to be seen as a function of the flow conditions (velocity and depth of the marine current). Of course, the effects of such a roughness are especially marked in lagoons, characterized by large expanses with low water depths of the order of one meter. In the presence of waves, the flow becomes periodic and the leaves follow the movements of the flow, maintaining quite similar oscillatory movements. Under these conditions, the effects that the plants have on the flow become difficult to identify as regards, for example, vertical velocity distribution, turbulence and energy dissipation.

The interaction between rigid vegetation and waves was analyzed by Lowe et al (2005), while Bradley and Houser (2009) focused their attention on the wave attenuation with flexible plants and wave motion, obtaining a significant wave height reduction. Results of such studies show that the wave height decay is well understood for submerged vegetation by adopting the exponential function proposed by Kobayashi et al (1993) and Mendez et al (1999), in which all the unconsidered aspects are embedded in the drag coefficient C_D, which is used to quantify the resistance of an object in the fluid environment.

Such a resistance is due to the skin friction on the surface of the kelp which could be affected by the viscous, turbulent and inertia effects. Previous studied have tried to link C_D with the Reynolds Number, which represents the ratio between turbulent and viscous forces, and the Keulegan-Carpenter number, which compares the horizontal water displacement under waves and the kelp dimension (see Kobayashi et al, 1993; Mendez et al, 1999; Koftis et al, 2013; Mendez and Losada, 2004; Bradley and Houser, 2009; Sanchez-Gonzalez et al, 2011; Houser et al, 2015; Cavallaro et al, 2010). The first coefficient allows to take into account the importance of flow turbulence. The second coefficient instead is specifically used for analyzing the effect of wave motion on the kelp.

More recently, Luhar and Nepf (2011, 2016) analyzed the dynamics of flexible blades induced by waves in order to explain the high dispersion of experimental data with respect to the above-mentioned parameters. Furthermore, Houser et al (2015) analyzed the influence of blade flexibility in the wave height attenuation over submerged meadows.

Several laboratory and field studies have been performed in order to estimate the flow induced by the waves inside a meadow (Luhar et al, 2010; Bradley and Houser, 2009; Luhar et al, 2013; Koftis et al, 2013). Such studies showed that a mean current is generated within a meadow under wave forcing and the orbital horizontal and vertical velocities are significantly decreased by the vegetation.

More recently, Wang et al (2016) studied the hydrodynamics due to waves and currents in the presence of vegetation. They showed that waves accelerate the flow velocity at the crest of the water surface, the turbulence intensity during the current-wave condition increases compared to current-only conditions and decreases due to the blocking effect of the vegetation.

The present work aims at collecting new information about the interaction between seagrass and waves by means of an experimental investigation. Such new experiments extend the preliminary studies of Cavallaro et al (2010) by carrying out new tests with several water levels and by also considering the blade flexibility in the analysis of results.

The paper is organized as follows. Section 2 presents the experimental setup. Section 3 shows the analysis related to the wave height dumping while Section 4 presents the results of the velocity attenuation inside the meadow. Concluding remarks are given in Section 5.

2 Experimental setup

The experiments have been carried out at the Hydraulics Laboratory of the University of Messina. The wave flume, shown in Figure 1, is about 18.00 m long, 0.42 m wide and 0.80 m high. Regular waves are generated by means of a flap-type wavemaker, which is driven by a pneumatic system and is electronically controlled. Moreover, a gravel absorbing beach, composed by marble stones with a median diameter D_{50}=3 cm, is placed at the opposite side of the flume, with a slope equal to 1:4.

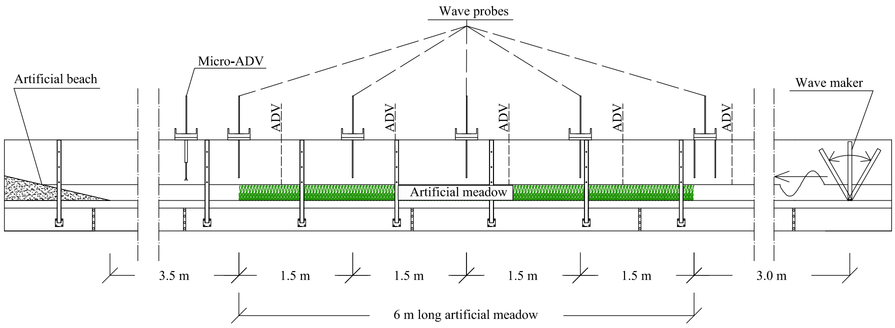

Fig. 1 Lateral view of the adopted experimental apparatus: wave channel with artificial meadow; the channel is equipped with an Acoustic Doppler Velocimeter (ADV) and wave probes.

The reference system is chosen in such a way that the x axis corresponds with the direction of wave propagation, the z axis is vertical and points upward (z = 0 at the bottom).

Inside the wave flume, a 6.0 m long synthetic meadow has been realized at a distance of 3.0 m from the wavemaker, such a length was enough to dissipate the evanescent standing waves generated by the wavemaker. Indeed, such waves are negligible after two or three water depth from the wavemaker (Dean and Dalrymple, 1992). The meadow is composed of artificial plants realized with low density polyethylene. Each artificial stem is composed of six leaves with the same width, equal to 0.01 m, and three different heights: 0.05 m, 0.10 m, and 0.20 m (see Figure 2). These plants are fixed to a metal plate in a regular grid with a density of 1,024 plants/m^2 (see Figure 3). This plant configuration reproduces the Posidonia Oceanica, which is an endemic plant

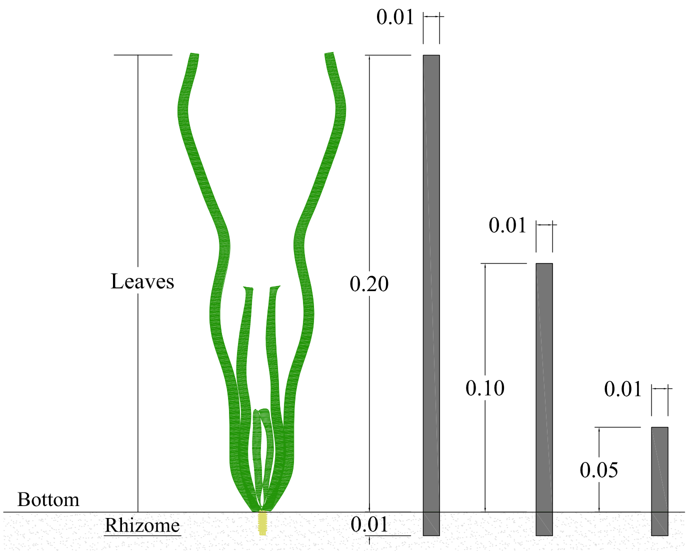

Fig. 2 Artificial plant used for the experiments: single stem made of 6 leaves (left), with three different lengths (right). All the dimensions are expressed in meters.

of the Mediterranean Sea. The polyethylene was chosen in order to reproduce the buoyancy and flexibility of real plants (see Cavallaro et al, 2010).

Five resistence wave gauges were placed across the meadow, at a mutual distance of 1.50 m. The wave gauge placed at the wavemaker side edge of the meadow was coupled with an additional gauge in order to estimate the wave reflection. Once collected from the wave gauges, the surface elevation data were post-processed in order to obtain the measured energy spectra, by using a Direct Fourier Transform (DFT) analysis. Then, the spectra of the incident and reflected waves were calculated by applying the Goda and Suzuki (1976) method. The knowledge of such energy spectra allows for the estimation of both the incident and the reflected wave heights (H_i and H_r respectively), and in turn of the reflection coefficient $K_r = H_r/H_i$. Such a coefficient falls

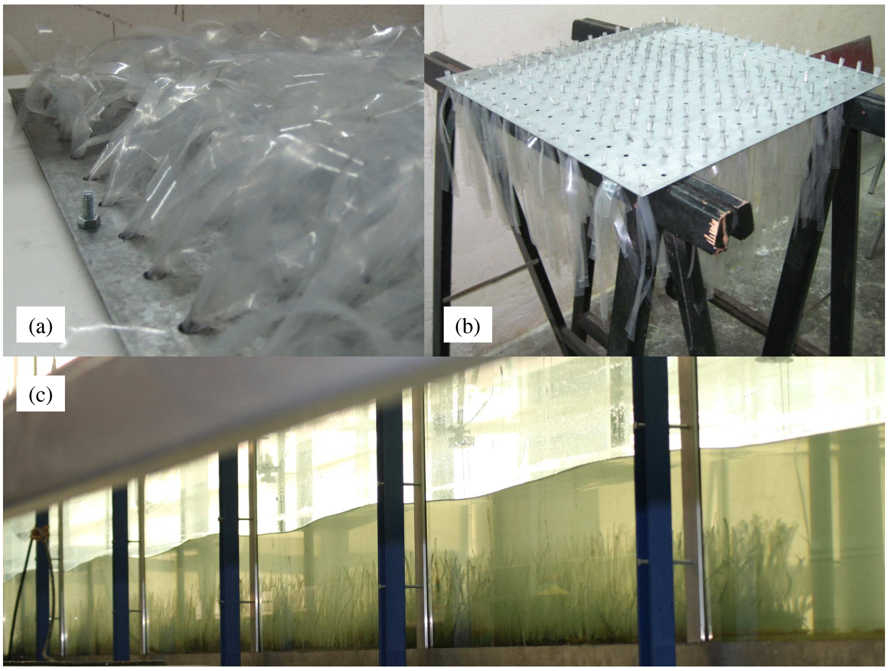

Fig. 3 Views of the tested artificial vegetation: (a) detail of the blades; (b) assembly of the model; (c) surface waves over the meadow.

within the range 0.10-0.15 for all the wave conditions which can be tested at the flume.

A Sontek Micro Acoustic Doppler Velocimeter (a 10 MHz ADV probe plus the ADVLab processor) is used to measure the three velocity components. The micro-ADV is located on a movable carriage, which allows to move the probe both horizontally and vertically. The sampling volume is a cylinder 9 mm high with a volume equal to 0.3 cm^3, located 5 cm far from the transmitter. The adopted sampling frequency is 30 Hz. During the experiments, the water temperature measured in the tank is quite constant, in the range 19°-21°C, therefore the value of the kinematic viscosity is assumed constant and equal to its value at 20°C, i.e., n = 1.0010^6 m^2/s. The obtained velocity profiles refer to the lower part of the water column, since no measurement can be taken between the wave crest and the level 5 cm below the wave trough. The mean velocity profiles were obtained by positioning the ADV in fixed point and by acquiring the velocity for at least 180 s.

The tests were carried out under regular waves characterized by heights in the range 0.020 - 0.135 m and periods in the range 0.6 - 1.6 s. Furthermore, the still water depth is in the range 0.29 - 0.45 m. It must be pointed out that wave periods longer than those indicated above cannot be reproduced without introducing too much disturbance, due to the limits imposed by the length of the wave flume.

3 Wave height reduction

3.1 Methodology

The presence of a meadow under progressive waves may cause energy reduction and wave height attenuation toward the direction of propagation. Such an effect is due to the mutual interaction between waves and leaves, which at the same time involves the movement of leaves and an increase of turbulence in comparison to the undisturbed orbital flow.

The approach adopted here for analyzing the wave height reduction is that proposed by Dalrymple et al (1984) and extended by Mendez and Losada (2004). Such an approach is applicable to any kind of plant, under arbitrary water depth and vertical extent of the leaves over the water column. All the unknown complex interactions between waves and plants are included in the drag coefficient C_D, which is assumed to be constant over the depth. That approach is valid for both rigid and flexible plants, since C_D can assume different values as a function of the flexibility of leaves.

The reduction of wave height H over the vegetation can be expressed as a function of the generic longitudinal distance x from the offshore boundary of the meadow:

$$K_v = \frac{H}{H_0} = \frac{1}{1 + \beta x} \tag{1}$$

where K_v is the damping coefficient; H_0 is the the incident wave height, registered at $x = 0$; β is a parameter independent from x and related to the characteristics of both waves and meadow.

Dalrymple et al (1984) derived β from the conservation of energy equation, by applying the linear wave theory. Similarly, Mendez and Losada (2004) obtained the following formula which is valid for monochromatic waves propagating over an horizontal bottom:

$$\beta = \frac{4}{9\pi} C_D b_v N H_0 k \frac{\sinh^3(k\alpha h) + 3\sinh(k\alpha h)}{[\sinh(2kh) + 2kh]\sinh(kh)} \tag{2}$$

where b_v is the plant area per unit height of each vegetation leaf perpendicular to the horizontal flow velocity, N is the number of vegetation stems per unit horizontal area, k is the wave number, h is the water depth, $\alpha = h_s/h$ is the relative plant height submergence ratio and h_s is the height of the leaves.

It is important to stress that the only dissipation term in eq. (2) is due to drag coefficient C_D, which contains all the neglected aspects in the interaction between waves and meadow: plant shape and flexibility, interaction between the leaves, length scale and amount of the turbulence induced by the meadow. Such neglected aspects should be taken into account in the choice of C_D.

A possible approach is to introduce several dimensionless parameters, which take into account the lacking phenomena of the wave-meadow interaction in eq. (2). Those parameters can be linked with C_D by means of empirical relations.

The parameter first adopted in the literature (see Kobayashi et al, 1993) is the Reynolds number defined as:

$$Re = \frac{b_v u_c}{\nu} \tag{3}$$

in which ν is the kinematic viscosity and u_c is a characteristic fluid velocity acting on the meadow, defined as the wave orbital velocity amplitude above the leaves. In particular, Mendez et al (1999) and Koftis et al (2013) suggest using the maximum velocity above the meadow, at its offshore edge:

$$u_c = \frac{\pi H_0}{T} \frac{\cosh(k\alpha h)}{\sinh(kh)} \tag{4}$$

Another parameter often related to C_D is the Keulegan-Carpenter number KC (see Mendez and Losada, 2004; Bradley and Houser, 2009; Sanchez-Gonzalez et al, 2011; Houser et al, 2015) which is the ratio of the length scale of oscillatory flow over the length scale of the vegetation:

$$KC = \frac{u_c T}{b_v} \tag{5}$$

Furthermore, a frequency parameter related to the interaction of a cylindrical element with an oscillatory flow can be applied (Sumer and Fredsoe, 1997; Scandura et al, 2009):

$$\beta_w = \frac{Re}{KC} = \frac{b_v^2}{\nu T} \tag{6}$$

The above mentioned parameters do not take into account the flexibility of the leaves since the only parameter related to the leaves is the average width b_v. Therefore, another dimensionless group is needed which also considers the slenderness and the elasticity of the leaves. Luhar and Nepf (2011) proposed the use of the Cauchy number (C_a), which is independent from C_D in oscillatory flows (see Luhar and Nepf, 2016):

$$Ca = \frac{\rho b_b u_c^2 l^3}{EI} \tag{7}$$

where ρ is the fluid density, b_b is the leaf width, l is the length of the leaf, E is the modulus of elasticity, I is the second moment of area for the leaf cross-section; $I = b_b t^3/12$ for rectangular cross-sections, where t is the thickness of the leaves .

The definition of the Cauchy number must be modified for the meadow with variable length of blades, since l is not unique. In particular, the relative occurence p_i of each generic length l_i must be considered. In this specific case, the lengths of blades are distributed uniformly among three different values: h_c , $h_c/2$ and $h_c/4$. Therefore p_i is always equal to 1/3 and term l^3 in eq. (7) becomes:

$$l^3 = \sum_{i=1}^{n} p_i l_i^3 = \frac{h_c^3}{3}\left(1 + \frac{1}{8} + \frac{1}{64}\right) \tag{8}$$

Houser et al (2015) proposed a parameter λ slightly different from Ca which is proportional to the rigidity of the blades rather than to their flexibility. The same variables are used in those parameters, thus they can be related under the assumption of blades with rectangular cross-sections:

$$\lambda = \frac{Et^3}{l^3 u_c^2} = \frac{12\rho}{Ca} \tag{9}$$

Such an equation highlights that λ and Ca are interchangeable for a given fluid, i.e. for fixed ρ. Only Cauchy number is used hereinafter, since it is dimensionless and assures a better generalization of the experimental outcomes.

3.2 Analysis of results

Wave heights registered during the experiments are used here for the estimation of the wave dumping related parameter β. Such a parameter is independent from the longitudinal abscissa inside the meadow but it is related to the meadow characteristics and to the wave conditions.

For each test, β is obtained by means of a best fit of eq. (1) applied to the observed wave heights. The capability of that relation in interpreting wave dumping is estimated by means of the normalized root mean square error of the coefficient K_v, defined as follows:

$$NRMSD(K_v) = \frac{1}{K_{v,max} - K_{v,min}} \sqrt{\frac{\sum_{i=1}^{n} \left(\hat{K_v} - K_v\right)^2}{n}} \tag{10}$$

where $K_{v,max}$ and $K_{v,min}$ are the maximum and minimum values of damping coefficient respectively; K_v is the value estimated from the measurements; $\hat{K_v}$ is the value predicted by means of the best fit for eq. (1); n is the number of sections over the meadow at which wave height has been measured. In the present experiments $n = 5$ since there are 3 wave gauges inside the meadow and 2 at its edge.

In order to assess the reliability of the acquired data, some preliminary analyses are performed. First, the coefficient β is estimated also by means of a simpler and more straightforward procedure, which takes into account only the wave heights at the edge of the meadow. In particualr, K_v and x are related only to the shoreward edge of the meadow and a unique value of β can be obtained from eq. (1). That methodology is quite coarse. Nevertheless, its results can be compared to those obtained by means of the best fit inside the meadow, in order to validate the adopted relationship for estimating the wave height reduction (i.e. eq. 1). The values of β obtained by means of the two methods are used, together with the incident wave characteristics, for estimating C_D for all the tests carried out.

In order to asses the reliability of eq. (1) in estimating wave dumping, a comparison is reported in Figure 4(a) between the results obtained from wave heights along the meadow and at its edge. Two tests show the greatest errors, with values of $NRMSD(K_v) \geq 0.25$. The same tests highlight also a mismatch between values of C_D estimated with the two methods described above, thus they have been excluded. Symmetrically, the tests with lower errors of K_v are those in which the two methodologies are more in accordance. Such a result confirms the reliability of the adopted formulation also when only data at the edge of the meadow are available, as in the experiments carried out

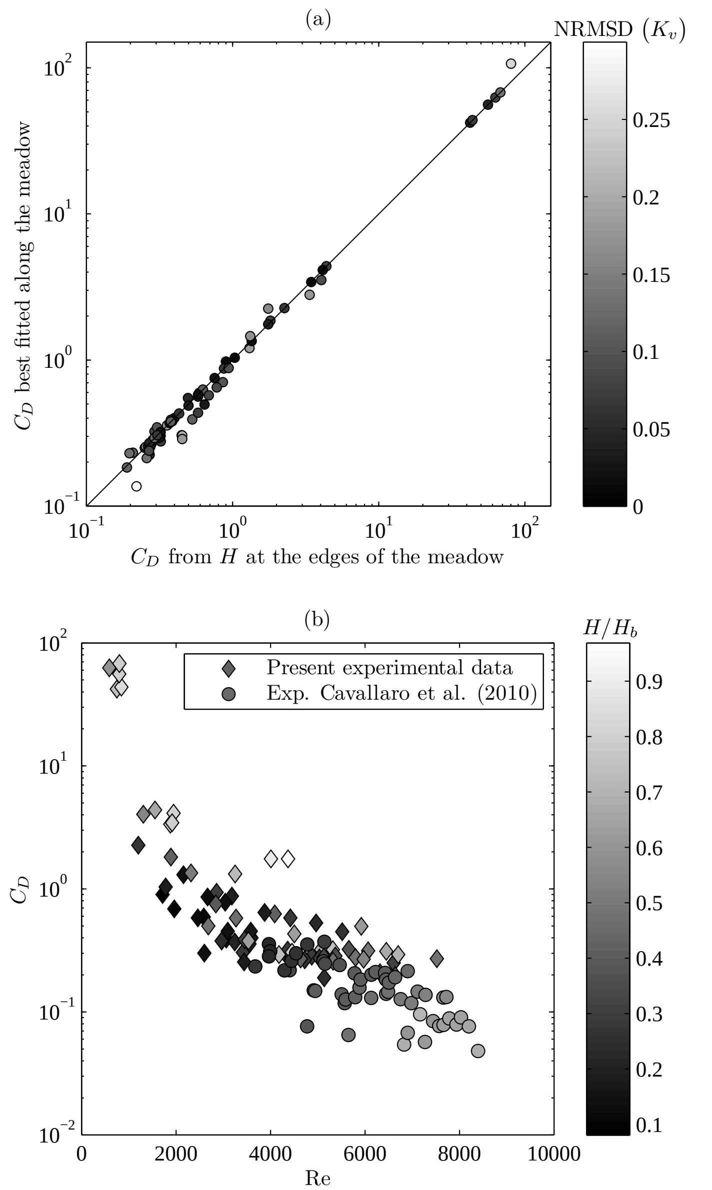

Fig. 4 Data analysis for the recognition of outliers: (a) comparison between drag coefficient C_D interpolated and at the edges of the meadow, gray intensity is related to the normalized root mean square error of K_v; (b) C_D as a function of Reynolds number Re for present and Cavallaro et al (2010) experiments, gray intensity is related to wave breaking ratio H/H_b.

previously by Cavallaro et al (2010) with the same artificial plants. Therefore, those experiments have also been taken into account in the present work.

A further preliminary analysis of data was carried out in order to compare the incident wave characteristics with the breaking limit value H_b proposed by Miche (1944):

$$\frac{H_b}{L} = 0.142 \tanh\left(\frac{2\pi h}{L}\right) \tag{11}$$

where L is the wave length obtained from the dispersion relation on the basis of the wave period T and the still water depth h.

Figure 4(b) shows C_D as a function of Re and breaking ratio H/H_b. Obviously, such a ratio is always lower than 1 since higher values would be physically impossible due to the activation of the wave breaking phenomenon. Nevertheless, values of H/H_b close to 1 highlight the presence of unstable near-breaking conditions or breaking phenomena underway. In those cases, wave dumping related coefficients (β and C_D) can be amplified independently from the meadow. In order to identify such conditions, a safe limit of H/H_b must be considered. Figure 4(b) shows that two tests furnish values of C_D and Re which are not in agreement with the trend of the remaining data and show amplified values of C_D. Such tests are slightly below the Miche's breaking limit since $H/H_b > 0.85$. Thus, they can be affected by breaking phenomenon and are excluded from the following analysis.

The methodology adopted for wave dumping estimation is valid for linear waves. Its limit is tested here by considering the effect of the nonlinear parameter L/h on the values of β obtained alternatively at the edge of the meadow

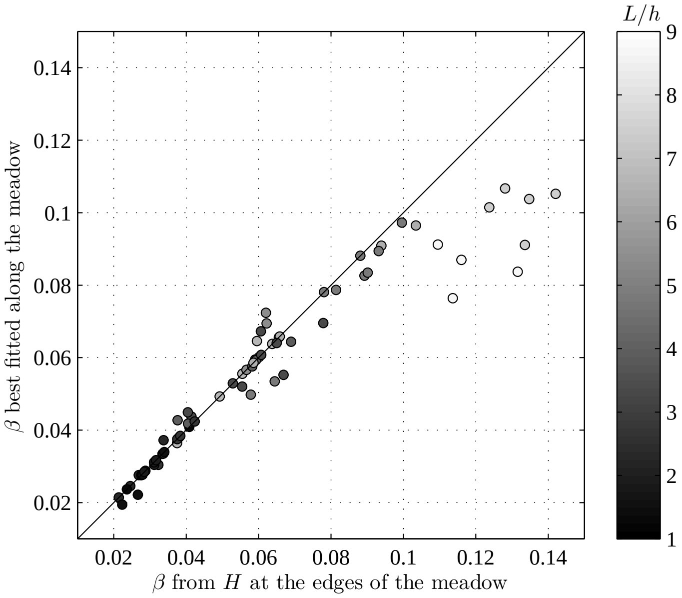

Fig. 5 Comparison between coefficient β obtained as interpolation over the horizontal position and at the edges of the meadow. The gray scale is a function of L/h.

and with the best fit along the meadow. Figure 5 shows that the two adopted methodologies provide similar values for $L/h < 7$. Such a threshold value corresponds to the shallow water limit proposed by Dingemans (1997): nonlinear models can be considered reliable above such a value. For non linear waves (i.e. $L/h \geq 7$), Figure 5 shows a deviation from the bisecting line. Therefore, the coefficients β obtained from the wave heights at the edges of the meadow are slightly overestimated in comparison to those obtained by means of the best fitting procedure. Such a result does not influence the reliability of the adopted methodology if best fitted data are taken into account. Furthermore,

Table 1 Values of coefficients a, b and c of eq. (12), proposed in the literature and in the present study.

Formula	a	b	c
Kobayashi et al (1993)	2200	2.40	0.080
Mendez et al (1999)	2200	2.20	0.080
Cavallaro et al (2010)	2100	1.70	0
Koftis et al (2013)	2400	0.77	0
Proposed formula	2550	3.05	0.095

the highlighted differences in β are less evident in the drag coefficient C_D, as shown in Figure 4.

The central role of C_D on wave-meadow interaction is confirmed by the number of past studies which have taken into account such a coefficient. The results obtained from the present tests are compared with experiments carried out in fairly similar conditions by Asano et al (1988), Cavallaro et al (2010) and Koftis et al (2013).

Figure 6 shows C_D as a function of Re for present and past experiments, from which a decreasing trend can be noted. A kind of formula which can fit those data is that proposed by Kobayashi et al (1993):

$$C_D = \left(\frac{a}{Re}\right)^b + c \tag{12}$$

where the coefficients a, b and c can be calibrated by means of experimental data. Table 1 summarizes the values of such coefficients in the formula proposed here and in similar relations from the literature.

The proposed formula is compared in Figure 6 with that proposed by Mendez et al (1999), which was calibrated on the basis of experiments of

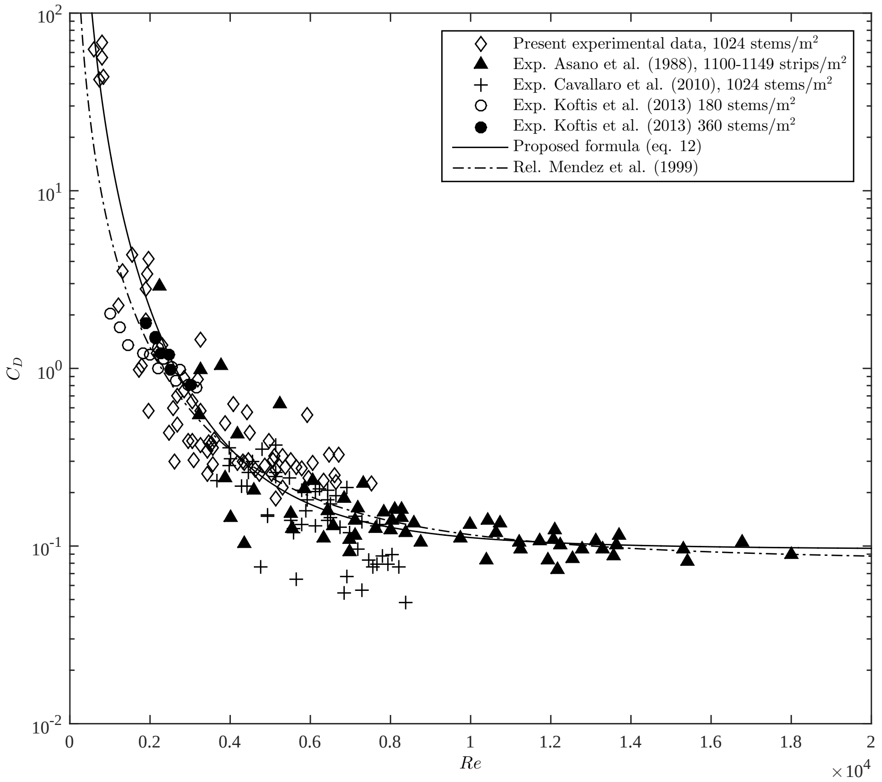

Fig. 6 Variation in drag coefficient C_D as a function of the Reynolds number Re; experimental data and empirical relations.

Asano et al (1988). Both formulas are able to describe fairly accurately the experimental data for $Re > 5000$, i.e. high Reynolds numbers. For $Re < 4000$, the proposed formulation provides a better match with the present experiments and with the experiments carried out by Koftis et al (2013) with a density of the meadow equal to 360 stems/m^2.

Flexibility of the blades is a common factor in the tests presented here and in the literature experiments cited above. The relationship between C_D and

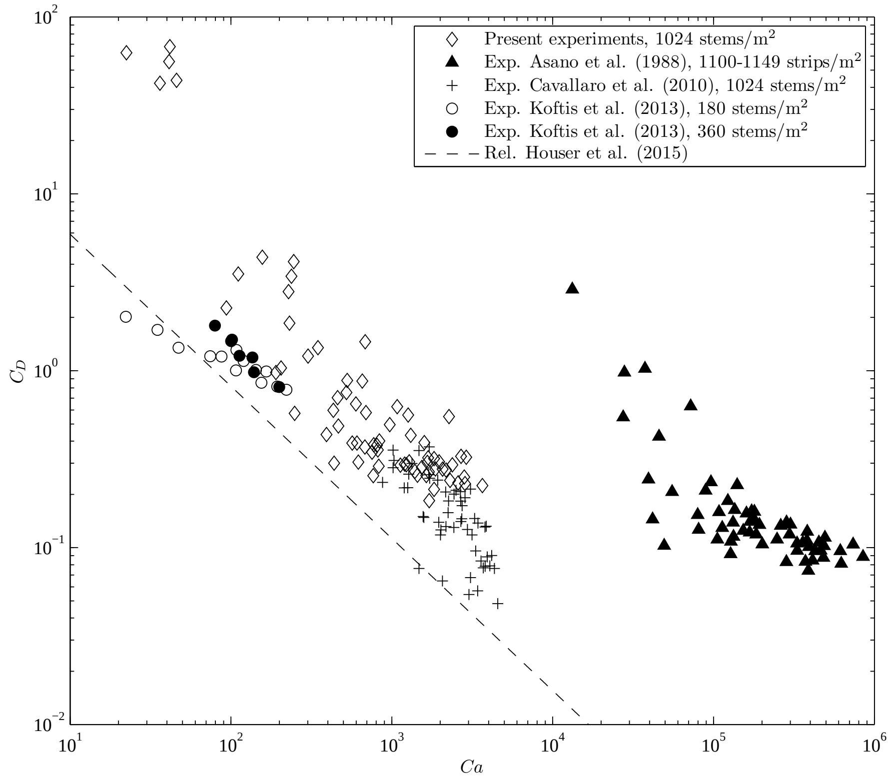

Fig. 7 Drag coefficient C_D as a function of the Cauchy number Ca, which takes into account blade flexibility.

Cauchy number Ca is shown in Figure 7 for all those tests. Such results do not highlight a clear trend, above all when the tests of Asano et al (1988) are considered. A possible reason is that the latter tests are related to very wide blades (i.e. $b_b = 5.2$ cm) which may cause stronger drag forces in comparison to the blades tested in all the other experiments taken into account, which have $b_b = 1$ cm.

The formula proposed by Houser et al (2015) is expressed as a function of the flexibility parameter λ, which can be related to Ca by considering the eq. (9), so becoming:

$$C_D = 0.0133\lambda^{0.86} = \left(\frac{79}{Ca}\right)^{0.86} \quad (13)$$

Such a formula represents in Figure 7 a lower boundary for the values of C_D considered here. That boundary is crossed by the large scale experiments of Koftis et al (2013) carried out with low density vegetation, i.e. 180 stems/m^2. The outcomes of the present experiments are far from the results of eq. (13) for the lowest values of Cauchy number, i.e. $Ca < 100$. If the experiments of Asano et al (1988) are excluded, a better agreement is found for $Ca > 100$.

An high variability of C_D is highlighted in both Figures 6 and 7, as a function of Re and Ca respectively. Therefore, the wave-meadow interactions must be investigated more in depth, in order to understand the rationale behind such a variability.

A new approach is proposed here which takes into account β_w, i.e. the ratio between Reynolds and Keulegan-Carpenter numbers. Such a variable is called 'frequency parameter' since it is related to the wave period (see eq. 6). That parameter is considered in Figure 8 together with Ca in order to investigate their simultaneous effect on C_D. The results are obtained for the present experiments and for the rehashed data of Cavallaro et al (2010) and show different trends for the same frequency parameter as a function of Ca: (i) C_D increases with β_w for small Cauchy numbers, i.e for light-gray symbols in Figure 8; (ii) C_D decreases with β_w for high values of Ca (dark-gray symbols).

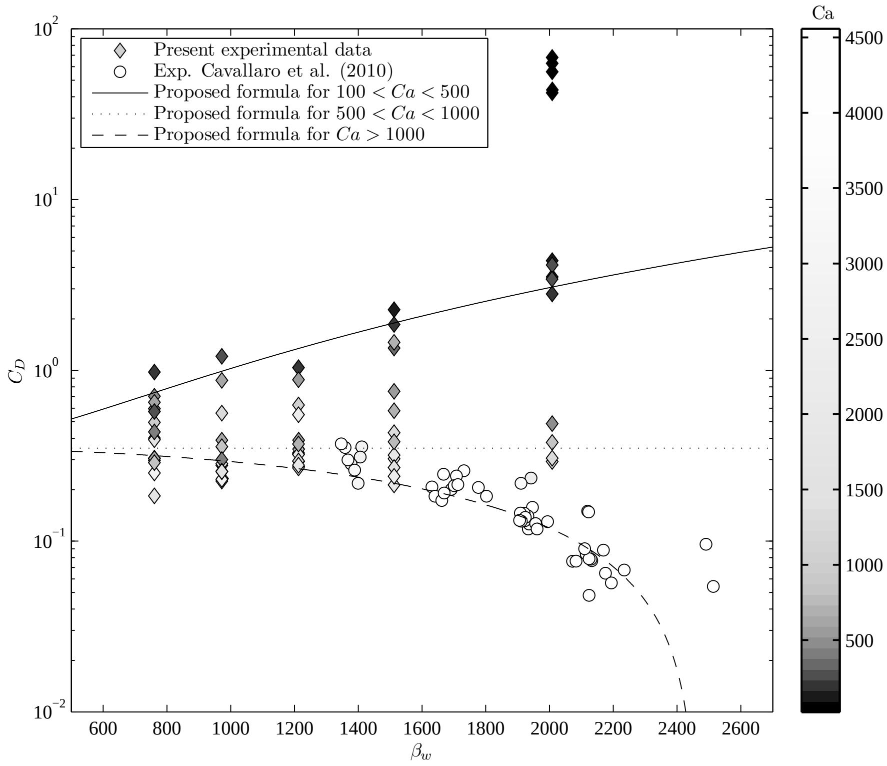

Fig. 8 Drag coefficient C_D as a function of the frequency parameter $\beta_w = b_v^2/(\nu T)$, for the present experiments and for the available data of Cavallaro et al (2010). Gray intensity is proportional to Cauchy number Ca; the trend lines are shown for three ranges of Ca.

Between these trends, a transition region is present for which drag coefficient is fairly constant.

The rationale behind such a dramatic change in trend can be found in the coupled effect of bending of blades and of wave frequency. The blades are close to the bottom when $Ca > 1000$, so the actual height of the meadow is lower than the length of the leaves, and the water column in which the flow interacts with the vegetation is smaller. In these conditions, the increase of frequency parameter β_w corresponds to lower values of the wave period which induce a reduction of orbital velocities inside the meadow, on the basis of the linear wave theory. On the whole, the reduction of inside-meadow velocities and the increase in bending of the meadow itself cause a reduction of interaction between waves and vegetation, in terms of drag coefficient.

Conversely, lower values of Cauchy number (i.e. $Ca < 500$) mean that the leaves are more rigid against the flow. If the frequency parameter increases in such conditions, the reduction of the wave period T causes a further tendency of the leaves to remain straight since the flow acts for a smaller time (equal to $T/2$) in one direction, after which it reverses. Essentially, the straighter the leaves, the greater the drag force. For the present experimental data, that effect is strongly amplified for very low values of orbital velocities, i.e. for $Re < 1000$ and $Ca < 100$. In such conditions, viscous forces dominate the interaction between waves and meadow and $C_D > 30$. It is important to stress that the latter conditions correspond to very low wave heights, which do not appreciably affect the coastal hydro-morphodynamics.

In order to highlight the different behaviors of C_D discussed above, three trend lines are shown in Figure 8, which have all the following form:

$$C_D = d\left(\beta_w\right)^2 + 0.35 \tag{14}$$

the coefficient d moves from positive to negative values with increasing C_a, as it is summarized in Table 2.

The lowest values of Cauchy number ($Ca < 100$) have been excluded from that analysis since those data are available only for high values of β_w. However,

Table 2 Proposed values of coefficient d in eq. (14) for classes of Cauchy number Ca.

Range	d
$100 < Ca < 500$	$6.8\ 10^{-7}$
$500 < Ca < 1000$	0
$Ca > 1000$	$-5.8\ 10^{-8}$

the results obtained by means of Re from eq. (12) are already satisfactory in those conditions, since such a range of Ca corresponds to the maximum of C_D in Figure 6 which is fitted adequately by means of that formula.

It is worth to point out that the eq. (14) differs from the eq. (12) since $C_D(\beta_w)$ may have an increasing trend (for $Ca < 500$). Conversely $C_D(Re)$ is always decreasing. Such a different behaviour is due to the fact that β_w is a function of the stem width and of the wave period, instead Re is also dependent on the wave height.

4 Velocity attenuation

According to the linear wave theory (Dean and Dalrymple, 1992), the horizontal and vertical velocity under a progressive wave propagating over a flat bottom is given by

$$u = \frac{\sigma H}{2} \frac{\cosh(kz)}{\sinh(kh)} \cos(kx - \sigma t) \tag{15}$$

$$w = \frac{\sigma H}{2} \frac{\sinh(kz)}{\sinh(kh)} \sin(kx - \sigma t) \tag{16}$$

where $\sigma = 2\pi/T$ is the wave radian frequency. It is worth recalling here that the vertical coordinate z is measured from the bottom of the flume. Such a description of the flow under progressive waves is obtained by assuming perfectly inviscid irrotational motion and by neglecting the nonlinear term in the Navier-Stokes equations.

The result of these assumptions is a flow with zero mean velocity. However, the observation of the flow field under a progressive wave shows non zero values on the mean horizontal velocity. Such a mass transport is generated by the non linear effect of wave propagation (Dean and Dalrymple, 1992) and by the effect of the flow viscosity for laminar flow (Longuet-Higgins, 1953) or turbulence asymmetry near the bottom (Scandura, 2007; Cavallaro et al, 2011).

More particularly, as first indicated by Starr (1947) the mass transport in the direction of waves propagation due to the non linear effect of wave propagation (the so called Stokes drift) is equal to:

$$M = \frac{E}{C} \tag{17}$$

where $E = \frac{1}{8}\rho g H^2$ is the wave total average energy per unit surface area, $C = \frac{L}{T}$ is the wave celerity, ρ is the water density, g is the gravitational acceleration, H is the wave height, L is the wavelength, and T is the wave period. Such a mass transport is concentrated in the region between the crest and the trough of wave (Dean and Dalrymple, 1992).

In a wave tank such a mass transport, co-directional with the wave direction, must be balanced by a mean current directed toward the wavemaker. This return current modifies the flow above and inside the meadow. An estimate of that return depth-averaged velocity could be obtained by means of the following relation:

$$U_t = \frac{M}{\rho h} \tag{18}$$

In the presence of a meadow, Luhar et al (2010) found that a mean current in the direction of wave propagation is generated within the meadow due to the non linear interaction with the oscillatory velocity. An estimate for the mean current generated within the meadow is:

$$U_{c,m} = \sqrt{\frac{4}{3\pi}\frac{C_{Dw}}{C_{Dc}}\frac{k}{\sigma}u_{w,m}^3} \tag{19}$$

where C_{Dw} and C_{Dc} are respectively steady and time-varying components of the drag coefficients, and $u_{w,m}$ is the magnitude of the in-meadow oscillatory flow.

Luhar et al (2010) found that the impact of the return current, due to both the stokes drift and the presence of the meadows, is negligible within the meadow. However, the present results show that the return current inside the meadow cannot be neglected and its value is greater than the mean current generated by the presence of the meadow (see Figure 9). Indeed, the time-averaged velocities inside the meadow show negative values and their mean value over the depth is close to U_t.

Regarding the velocity structure, Koftis et al (2013) reported that inside the meadow the orbital horizontal and vertical velocities are significantly decreased. During the present experiments six velocity profiles were detected: two outside the meadows and four inside the meadow. The results of the present experiments show a strong correlation between the wave height dumping and the velocity dumping due to the presence of the meadow.

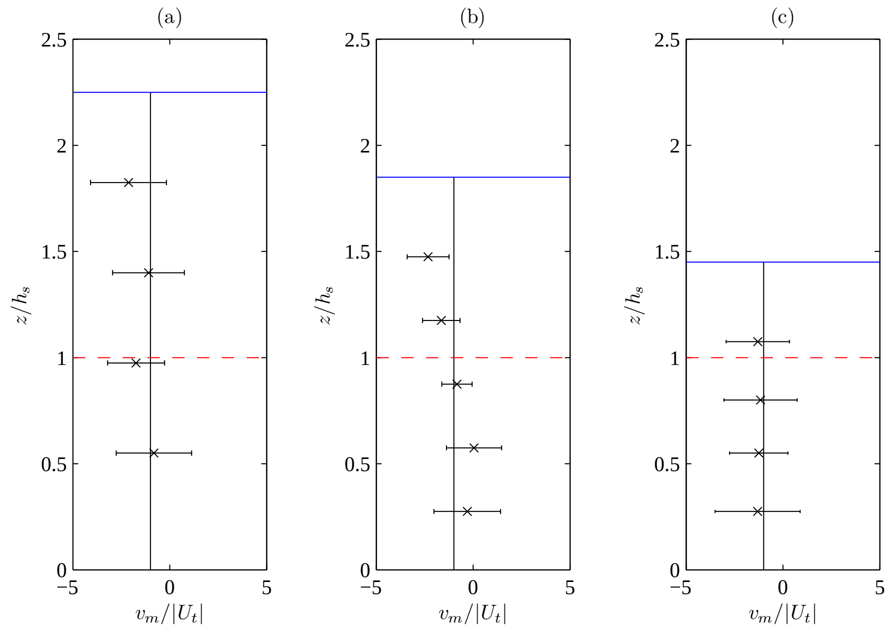

Fig. 9 Profiles of average velocities v_m over the mass transport velocity from linear theory $|U_t|$: (a) high water depth condition; (b) intermediate water depth; (c) small water depth. Dashed line is the maximum height of the meadow.

As shown in Figure 10 for the two tests, the velocity profiles along the meadow are close to those evaluated by the linear wave theory in which the local wave height is adopted. Such a local height is defined as that evaluated at the same section where the velocity profile is registered. Therefore, the velocity provided by the linear wave theory is coupled with the return current generated by the Stokes drift. The same analysis is carried out for all the tests.

Figure 11 shows the amplitude of the registered orbital horizontal velocities versus the values of the corresponding variable evaluated by means of the linear wave theory. Such a figure demonstrates that the correlation between

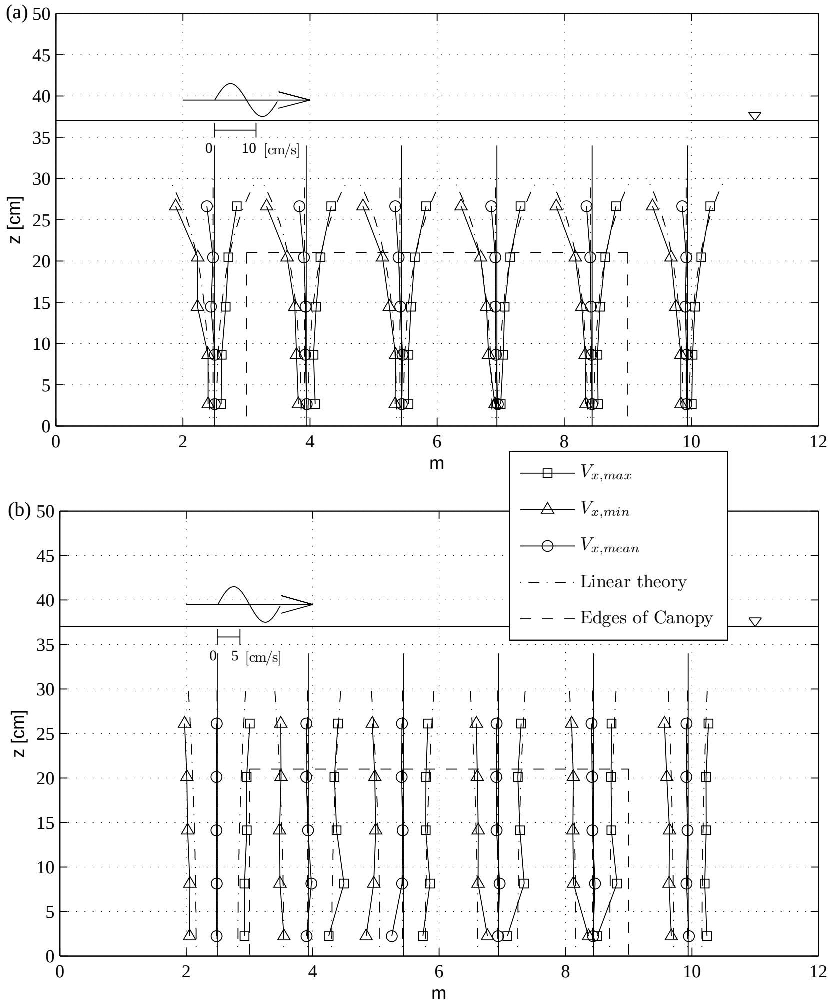

Fig. 10 Horizontal velocity profiles measured and predicted from the linear wave theory for to tests carried out with still water depth $h = 0.37$ m: (a) incident waves having $H = 0.04$ m, $T = 0.6$ s; (b) incident waves having $H = 0.04$ m, $T = 1.6$ s.

the amplitude of the orbital velocity and the local wave height is substantially independent from the vertical and horizontal position along the meadow.

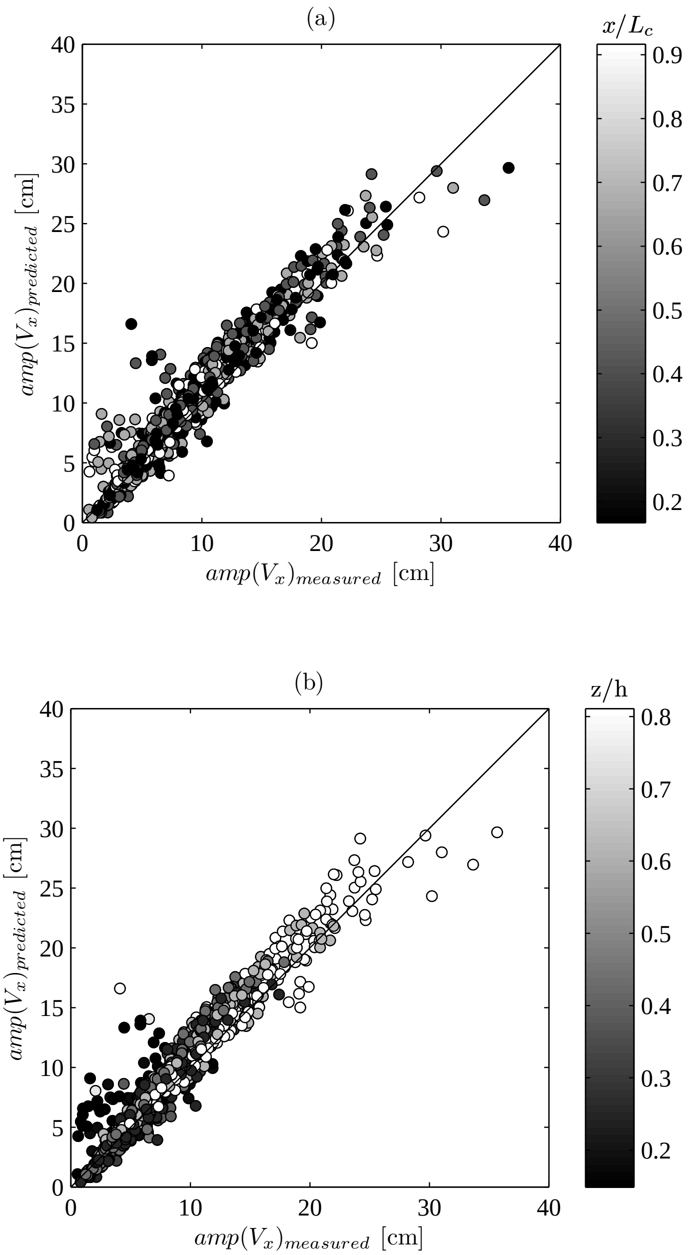

Fig. 11 Orbital velocity amplitudes measured and predicted from the linear wave theory.

5 Conclusions

The interaction between a meadow and surface waves involve complex hydrodynamics related to both incident wave conditions and flexibility of the leaves. By means of physical modeling, two main effects of such an interaction are considered in the present work: wave height reduction and velocity profile modification in comparison to the linear wave theory.

The experiments were carried out for a dense meadow composed of polyethylene blades, in which flexibility played a key role.

The analysis of the drag coefficient as a function of the Reynolds number confirms a decreasing trend widely investigated in the literature by means of a power law. The relevant number of experiments, carried out in the present work in a wide range of Re, further improves that existing formula with a focus on flexible leaves with high density.

Leaf flexibility effect on the wave dumping is analyzed by a direct comparison between Cauchy number and drag coefficient. An existing formulation is shown to represent a lower limit for the test carried out. Nevertheless, the values of C_D are dramatically underestimated by that formulation, especially for small values of Ca.

Furthermore, a coupled analysis of the results is performed as a function of Cauchy number and frequency parameter. Such an analysis highlights the presence of very different behaviours for three classes of Ca: (i) C_D increases with the wave frequency for small values of Cauchy number, i.e. for Ca < 500; (ii) C_D assumes a nearly constant value for $500 < Ca < 1000$; (iii) C_D decreases as a function of β_w for highly flexible leaves ($Ca > 1000$). Therefore, the change of flexibility modifies the response of the leaves to the waves. In particular, the leaves have a small tendency to bend for small values Ca. In these conditions, an increase in wave frequency causes a reduction of the period in which the flows act in one direction. Thus, the leaves are straight for a longer time and the drag coefficient increases dramatically. On the other hand, the leaves are unable to stay vertical for very large values of Ca and are always bent toward the bottom, independently from the wave conditions. In such cases, an increase in wave frequency causes a reduction of the orbital waves near to the bottom and of the interactions between waves and leaves.

A reduction of wave height is expected to cause a decrease in orbital velocity. The comparison of the registered amplitude of waves inside the meadow with the values predicted by the non linear theory have a fairly good match, if the dumped wave height is used. Therefore, the amplitude of orbital velocity does not highlight a clear variation along the water depth due to the presence of the seagrass and its reduction is mainly related to the horizontal position along the seagrass.

Furthermore, the mean velocities inside the meadow are lower than those evaluated above the leaves. Such behavior is probably due to the current generated inside the meadow due to the interaction between the leaves and the oscillatory velocity.

Acknowledgements This work has been partly funded by the EU funded project HYDRALAB PLUS (proposal number 64110).

References

Asano T, Tsutsui S, Sakai T (1988) Wave damping characteristics due to seaweed. In: Proe. 35th Coast. Engrg. Conf. in Japan, Japan Society of Civil Engineers (JSCE), pp 138 –142, (in Japanese)

Bouma TJ, De Vries MB, Low E, Peralta G, Tnczos IC, van de Koppel J, Herman PMJ (2005) Trade-offs related to ecosystem engineering: A case study on stiffness of emerging macrophytes. Ecology 86(8):2187–2199, DOI 10.1890/04-1588

Bradley K, Houser C (2009) Relative velocity of seagrass blades: Implications for wave attenuation in low-energy environments. Journal of Geophysical Research: Earth Surface 114(F1), DOI 10.1029/2007JF000951, f01004

Carpenter SR, Lodge DM (1986) Effects of submersed macrophytes on ecosystem processes. Aquatic Botany 26:341 – 370, DOI 10.1016/0304-3770(86)90031-8, submerged Macrophytes: Carbon Metabolism, Growth Regulation and Role in Macrophyte-Dominated Ecosystems

Cavallaro L, Re CL, Paratore G, Viviano A, Foti E (2010) Response of Posidonia Oceanica to wave motion in shallow-waters - preliminary experimental results. In: Proceedings of the 32nd International Conference on Coastal Engineering, 32, p 49, DOI 10.9753/icce.v32.waves.49

Cavallaro L, Scandura P, Foti E (2011) Turbulence-induced steady streaming in an oscillating boundary layer: On the reliability of turbulence closure models. Coastal Engineering 58(4):290–304

Dalrymple RA, Kirby JT, Hwang PA (1984) Wave diffraction due to areas of energy dissipation. Journal of Waterway, Port, Coastal, and Ocean Engineering 110(1):67–79, DOI 10.1061/(ASCE)0733-950X(1984)110:1(67)

Dean RG, Dalrymple RA (1992) Water Wave Mechanics for Engineers and Scientists. World Scientific

Dingemans M (1997) Wave propagation over uneven bottoms. Advanced Series on Ocean Engineering 13, World Scientific, Singapore, ISBN 981-02-0427-2.

Goda Y, Suzuki T (1976) Estimation of incident and reflected waves in random wave experiments. In: Proceedings of 15th Conference on Coastal Engineering, Honolulu, Hawaii, 1976, pp 828–845

Houser C, Trimble S, Morales B (2015) Influence of blade flexibility on the drag coefficient of aquatic vegetation. Estuaries and Coasts 38(2):569–577, DOI 10.1007/s12237-014-9840-3

John BM, Shirlal KG, Rao S, Rajasekaran C (2016) Effect of artificial seagrass on wave attenuation and wave run-up. The International Journal of Ocean and Climate Systems 7(1):14–19, DOI 10.1177/1759313115623163

Kobayashi N, Raichle AW, Asano T (1993) Wave attenuation by vegetation. Journal of Waterway, Port, Coastal, and Ocean Engineering 119(1):30 – 48, DOI 10.1061/(ASCE)0733-950X(1993)119:1(30)

Koch EW, Sanford LP, Chen SN, Shafer DJ, Mckee SJ (2006) Waves in seagrass systems: review and technical recommendations. techreport ERDC TR-06-15, US Army Corps of Engineers

Koftis T, Prinos P, Stratigaki V (2013) Wave damping over artificial posidonia oceanica meadow: A large-scale experimental study. Coastal Engineering 73:71 – 83, DOI 10.1016/j.coastaleng.2012.10.007

Lakshmanan N, Kantharaj M, Sundar V (2012) The effects of flexible vegetation on forces with a keulegan-carpenter number in relation to structures due to long waves. Journal of Marine Science and Application 11(1):24–33, DOI 10.1007/s11804-012-1102-9

Longuet-Higgins MS (1953) Mass transport in water waves. Philosophical Transactions of the Royal Society of London A: Mathematical, Physical and Engineering Sciences 245(903):535–581, DOI 10.1098/rsta.1953.0006

Lowe RJ, Koseff JR, Monismith SG (2005) Oscillatory flow through submerged canopies: 1. velocity structure. Journal of Geophysical Research C: Oceans 110(10):1–17

Luhar M, Nepf H (2016) Wave-induced dynamics of flexible blades. Journal of Fluids and Structures 61:20 – 41, DOI 10.1016/j.jfluidstructs.2015.11.007

Luhar M, Nepf HM (2011) Flow-induced reconfiguration of buoyant and flexible aquatic vegetation. Limnology and Oceanography 56(6):2003–2017, DOI 10.4319/lo.2011.56.6.2003

Luhar M, Coutu S, Infantes E, Fox S, Nepf H (2010) Wave-induced velocities inside a model seagrass bed. Journal of Geophysical Research: Oceans 115(C12), DOI 10.1029/2010JC006345, c12005

Luhar M, Infantes E, Orfila A, Terrados J, Nepf HM (2013) Field observations of wave-induced streaming through a submerged seagrass (posidonia oceanica) meadow. Journal of Geophysical Research: Oceans 118(4):1955–1968

Mendez FJ, Losada IJ (2004) An empirical model to estimate the propagation of random breaking and nonbreaking waves over vegetation fields. Coastal Engineering 51(2):103 – 118, DOI 10.1016/j.coastaleng.2003.11.003

Mendez FJ, Losada IJ, Losada MA (1999) Hydrodynamics induced by wind waves in a vegetation field. Journal of Geophysical Research: Oceans 104(C8):18,383–18,396, DOI 10.1029/1999JC900119

Miche R (1944) Mouvements ondulatoires de la mer en profondeur constante ou decroissante. Annales des Ponts et Chaussees 114:25–78, 131–164, 270–292, 369–406, (in French)

Peralta G, Brun FG, Prez-Llorns JL, Bouma TJ (2006) Direct effects of current velocity on the growth, morphometry and architecture of seagrasses: A case study on zostera noltii. Marine Ecology Progress Series 327:135–142

Sanchez-Gonzalez JF, Sanchez-Rojas V, Memos CD (2011) Wave attenuation due to posidonia oceanica meadows. Journal of Hydraulic Research 49(4):503–514, DOI 10.1080/00221686.2011.552464

Scandura P (2007) Steady streaming in a turbulent oscillating boundary layer. Journal of Fluid Mechanics 571:265–280

Scandura P, Armenio V, Foti E (2009) Numerical investigation of the oscillatory flow around a circular cylinder close to a wall at moderate keulegancarpenter and low reynolds numbers. J Fluid Mech 627, DOI 10.1017/S0022112009006016

Starr VP (1947) A momentum integral for surface waves in deep water. Journal of marine Research 6(2)

Sumer B, Fredsoe J (1997) Hydrodynamics Around Cylindrical Structures. Advanced series on ocean engineering, World Scientific

Wang X, Xie W, Zhang D, He Q (2016) Wave and vegetation effects on flow and suspended sediment characteristics: A flume study. Estuarine, Coastal and Shelf Science 182:1 – 11, DOI 10.1016/j.ecss.2016.09.009